Carbohydrate Polymers 117 (2015) 25–33

Contents lists available at ScienceDirect

Carbohydrate Polymers

journal homepage: www.elsevier.com/locate/carbpol

In vitro release of theophylline from starch-based matrices prepared *via* high hydrostatic pressure treatment and autoclaving

Wioletta Błaszczak[a,*], Adam Buciński[b], Adrian R. Górecki[a]

[a] Institute of Animal Reproduction and Food Research of Polish Academy of Sciences, Tuwima 10, 10-748 Olsztyn, Poland
[b] Nicolaus Copernicus University Collegium Medicum, Jagiellońska 13-15, 85-067 Bydgoszcz, Poland

ARTICLE INFO

Article history:
Received 28 May 2014
Received in revised form 28 August 2014
Accepted 1 September 2014
Available online 28 September 2014

Keywords:
High pressure
Starch
Theophylline
Release profile
Kinetic models
Surface area

ABSTRACT

Recent works have demonstrated that release behavior of bioactive compounds varies with the nature of the matrix regarding its chemical composition, morphology and surface properties. Starch matrices varying in amylose content (maize, sorghum, Hylon VII) or pure amylopectin ones (waxy maize, amaranth starch), containing theophylline (10 mg, 50 mg/0.5 g of starch), were obtained *via* high hydrostatic pressure treatment (650 MPa/9 min) and autoclaving (120 °C/20 min). Both the treatment used and drug dose affected the theophylline release profiles from the matrices studied. The profiles of amylopectin starch matrices satisfactorily fitted with selected mathematical models, indicating a controlled theophylline release. The principal component analysis confirmed substantial differences in drug release between the amylose and amylopectin matrices. The differences in matrix morphology, internal surface area and porosity (mesopore diameter, cumulative pore volume) between the matrices studied were found to be key factors affecting the theophylline dissolution.

1. Introduction

As a biodegradable polymer with simple and well-defined chemical properties, starch is widely used in the food and non-food industry. To meet steadily increasing demands for improved specific starch properties, its granules are subjected to chemical or physical treatment (Pei-Ling, Qing, Qun, Xiao-Song, & Ji-Hong, 2012). Starch and its derivatives were successfully adopted to develop carriers for bioactive compounds or as a matrices/hydrogels for controlled drug delivery (Lopez-Cordoba, Deladino, & Martino, 2014; Xiao, 2013; Nair & Jyothi, 2013; Ismail, Irani, & Ahmad, 2013). Among different modifications and derivatization methods applied to produce new starch material from native granules, high hydrostatic pressure (HP) has attracted much attention as a non-thermal processing technology (Pei-Ling et al., 2012).

Although, HP has been defined as a "mild technology", it yields effective changes in the structure and in the physicochemical properties of starch granules (Pei-Ling et al., 2012). Starches composed of mainly amylopectin when subjected to HP treatment in excess of water was capable of forming an amorphous, three-dimensional network structure (Błaszczak, Wasserman, Fornal, & Yuryev, 2007). On the contrary, starches with medium and high concentration of amylose maintained their granular shape under HHP and demonstrated limited swelling and amylose release (Vallons & Arendt, 2009). The susceptibility (rate and degree) of HP-treated starches to retrogradation, their resistance to enzymatic activity or swelling power may differ significantly from those properties displayed by heat-gelatinized granules (Pei-Ling et al., 2012).

Hydrophilic matrices, including starch hydrogels produced *via* HP (Szepes et al., 2008) or these obtained by hydrothermal treatment and subsequent retrogradation (Yoon, Lee & Lim, 2009) have been recognized as interesting material for application in drug release formulation. They may be used for controlled release of both water-soluble and water-insoluble active compounds (Bialleck & Rein, 2011; Nair & Jyothi, 2013).

Theophylline as a model drug has been widely analyzed in various release systems (tablet, capsule, solution) since it demonstrated almost constant solubility (1 g/120 mL) in a wide range of pH values (Yoon et al., 2009). Since theophylline manifested narrow therapeutic range, it is crucial to investigate the differences in release rate of this drug between formulations (Wolny, Gruchlik, Chodurek, Szara, & Dzierżewicz, 2012). Recent works have demonstrated that the release behavior of theophylline varies with the nature of the matrix, and can be controlled among others through its chemical composition, method of formulation used and/or its physical properties (Nair & Jyothi, 2013).

* Corresponding author. Tel.: +48 89 523 46 15; fax: +48 89 524 01 24.
E-mail addresses: w.blaszczak@pan.olsztyn.pl (W. Błaszczak), kizbiofarmacji@cm.umk.pl (A. Buciński), a.gorecki@pan.olsztyn.pl (A.R. Górecki).

http://dx.doi.org/10.1016/j.carbpol.2014.09.031
0144-8617/

Ultrahigh hydrostatic pressure as an attractive physical process was also applied to formulate the main starch carrier for theophylline (Szepes et al., 2008). The potato (PS) and maize (MS) starches containing theophylline were treated with 700 MPa for 5 min in order to evaluate (*in vitro)* their effectiveness in drug delivery behavior. The release mechanism of theophylline from the starch-based matrices was characterized with different empirical models. The mechanism that regulates the release behavior of an active substance from the polysaccharide matrices involves such complex processes as: swelling, wettability, diffusion, biodegradation (erosion) processes, and their interactions (Nair & Jyothi, 2013). According to Szepes and co-authors, the release of theophylline from PS best fitted to the Hixon–Crowel model indicating that the drug release occurred only in vertical direction relative to matrix surface. However, the release of theophylline from MS matrices was best explained by the Krosmeyer–Peppas kinetics signifying that the theophylline release was governed by non-Fickian diffusion. This phenomenon was ascribed by the authors to the simultaneous water uptake during drug diffusion, which in turn affected matrix relaxation.

Little information is available in literature regarding applicability of HP and use of other types of starch *i.e.* with unique physicochemical properties (amaranth and sorghum starches) (Błaszczak, Misharina, Fessas, Signorelli, & Gorecki, 2013), or starches with complex polymorph structure (Hylon VII) to obtain novel material with suitable properties for drug release.

In this study the following starches: waxy maize and amaranth starch (composed of almost 100% amylopectin), maize and sorghum (~20% of amylose) as well as Hylon VII (68% of amylose), were evaluated as the main and potential carriers of theophylline. Theophylline as a model drug (at low and high drug content) was used to characterize drug delivery behavior from starch matrices prepared *via* hydrothermal (autoclaving, 121 °C, 0.1 MPa, 20 min) and non-thermal (HHP, 650 MPa, 9 min, 30 ± 2 °C) treatment. An *in vitro* study was conducted in order to determine kinetic parameters by fitting experimental data to selected mathematical models.

2. Materials and methods

2.1. Materials

Seeds of plant species *Amaranthus cruentus L.* were donated by the Metro Industrial Centre "Szarłat" s.c. (Łomża, Poland), and grains of *Sorghum bicolor* (v. Rona 1) were purchased from the Kutno-Centre for Sugar Beet Breeding in Straszkow, Poland.

The starch from amaranth seeds was isolated and purified according to the method developed by Walkowski, Fornal, Lewandowicz, and Sadowska (1997). Because amaranth starch granules (pure amylopectin starch) naturally form agglomerates that vary in diameter, the isolated starch granules were sieved through a screen with a mesh of 350—in order to unify their diameters.

The isolation procedure described by Olayinka, Adebowale, and Olu-Owolabi (2008) was used to obtain starch from sorghum grains (19.2% of amylose).

The other experimental materials were Hylon VII starch (68% of amylose), refined from high amylose maize (The National Starch & Chemical Co.), waxy maize starch (trace amounts of amylose) (Sigma, S-9679), and commercial maize starch (20.5% of amylose) which was donated by the Department of Food Concentrates in Poznan, the Institute of Agricultural and Food Biotechnology, Poland.

Since in our previous work these starches were fully characterized regarding their chemical composition (Błaszczak et al., 2013), the results were not presented herein.

Anhydrous theophylline (min. 99%, T-1633) was purchased from Sigma.

2.2. Sample preparation

Starch–water suspensions (3 g dm/10 mL) containing solubilized theophylline at the concentration of 10 mg and 50 mg (per 0.5 g dm of starch) were thoroughly mixed and homogenized with a Polytron Ultraturrax homogenizer IKA-T18 (IKA works, Wilmington, USA) for 1 min at 12,000 rpm.

2.2.1. Pressure treatment

The sample prepared was closed in a teflon tube (50 mL), thoroughly mixed, deaerated, closely sealed and subjected to HHP treatment using a high pressure device type Unipress U-303 (Warsaw, Poland). The teflon tube was put into a high pressure chamber (with the capacity of approximately 100 mL) filled with a pressure-transmitting medium which also minimized adiabatic heating. The samples were pressure-treated at 650 MPa for 9 min. The time needed to reach the working pressure was 2 min. The temperature inside the pressure chamber averaged 30 ± 2 °C. The pressure treatment was performed in two repetitions for each combination.

2.2.2. Autoclaving

For autoclaving the sample was closed into Pyrex® bottle (with cap and pouring ring), and pre-treated according to the method given by Yoon et al. (2009). In order to prevent the phase separation during autoclaving, the sample was heated in a water bath (70 °C/80 s), and then autoclaved (121 °C/20 min, 0.1 MPa) using a vertical steam sterilizer (type ASV, SMS Warsaw, Poland).

After the pressure treatment and autoclaving the starch matrices containing theophylline were frozen in liquid nitrogen, freeze-dried, grinded in a laboratory grinder (Sadkiewicz Instruments®, Poland) and sieved through a screen with a mesh of 170—in order to unify their diameters. The starch matrices were sealed in tubes and stored in a dark, cold and dry place until the analysis.

For better clarity, the following code of preparations has been proposed:

- *for starches*: maize starch (MS), sorghum starch (SS), Hylon VII (Hylon), waxy maize starch (WMS), and amaranth starch (AS);
- *for processing*: high pressure treatment (HP) and autoclaving (STR);
- *for theophylline* (T_f) concentration: 10 mg/0.5 g starch (T_{f10}), 50 mg/0.5 g starch (T_{f50}).

2.3. In vitro release studies

Each of starch preparations containing T_f was weighed on laboratory microbalance (Sartorius ME36S-OCE, Sartorius AG Germany) into eight gelatin capsules (B&E, Poland) in an amount of 100 mg.

The amount of T_f released from each capsule was evaluated over a 4-h period using an Erweka DT800 dissolution tester (Erweka GmbH, Germany). The test was accomplished by transferring 900 mL of purified water (Millipore, USA) to 6 dissolution vessels and the temperature was maintained at 37 ± 0.5 °C. One capsule was placed in each rotating basket within each vessel to begin the dissolution test at 50 rpm. In all the experiments, 6 mL of dissolution samples were collected from the vessels at: 5, 10, 15, 30, 45, 60, 90, 120, 150, 180, 210, 240 min and replaced with an equal volume to keep them submerged. A correction factor was included in the calculations to account for the drug lost in the sample. All determinations of T_f concentration and calibration curve were carried out using a UV-2501 PC spectrophotometer (SHIMADZU Corporation, Japan) at `λ = 273 nm. The calibration curve was plotted from

eight dilutions with a concentration range of 0.078–12.00 mg/L of T_f in purified water. The equations of calibration curve were estimated using linear regression analysis and correlation coefficient (R) was calculated. During the validation process, the curve had a correlation coefficient greater than 0.999.

2.4. Mechanism of T_f release

The T_f release profile data was analyzed for compliance with mathematical models of drug dissolution using the non-linear estimation function (Statistica 10). Selected kinetic models, having the highest correlation coefficient (R value), are presented:

- First-order model: $Q_t/Q_{max} = 1 - \exp(-kt)$
- Higuchi square root time model: $Q_t/Q_{max} = kt^{0.5}$
- Hixson–Crowell model: $1 - Q_t/Q_{max} = 1 - kt$
- Korsmeyer–Peppas model: $Q_t/Q_{max} = kt^n$

where Q_t is the amount of drug released in time t, Q_{max} is the initial drug amount, k is the release rate constant and n is the diffusional exponent (Szepes et al., 2008).

2.5. Surface properties and morphology of starch matrices

2.5.1. Low-temperature nitrogen adsorption

The specific surface area and average mesopore diameter of HP treated and STR matrices without T_f addition were estimated using low-temperature nitrogen adsorption (ASAP 2405, Micrometrics Inc., USA). Isotherms were plotted for high-purity nitrogen adsorption at a temperature of 77.3 K. The monolayer capacity was calculated on the basis of adsorption isotherm (Brunauer, Emmett, & Teller, 1938) from five measurement points in the relative pressure range p/p_0 0.006–0.2. Prior to the measurements, starch samples were dried for 25 h in vacuum at 100 °C, automatically desorbed and flushed with pure helium. Pore characteristics (diameter and cumulative pore volume) was determined according to the desorption method of Barrett, Joyner, and Hallenda (1951) (BJH model). Samples were analyzed in triplicate.

2.5.2. Scanning electron microscopy

The starch pastes/gels (without T_f addition) obtained after treatment (HP, STR) were frozen in liquid nitrogen and freeze-dried. The cross-section was used to analyze the internal structure of a starch matrix. Finally, the sectioned parts were stuck on a specimen holder using a silver plate, and then coated with gold in a vacuum evaporator (JEE 400, Jeol, Japan). The specimens obtained were viewed in a scanning electron microscope (Jeol JSM 5200, Japan) at an accelerating voltage of 10 kV.

2.6. Statistical analysis

Kinetica v.5.0 (Thermo Fisher Scientific) software was used to determine the parameters characterizing the active ingredient release. All obtained data were subjected to statistical analysis using Statistica v.10 (StatSoft Inc., USA). The data was checked for normality of distribution using the Shapiro–Wilk test. The first step of the statistical analysis was determining statistically significant differences between the release parameters designated for all prepared granulates. The parameter of the release profiles was assessed using ANOVA *post-hoc* LSD test (IBM SPSS Statistics 20 software). The PCA results were graphically represented by the projection of the first two principal components using the correlation matrix type (MINITAB® Statistical Software v.16.1.1). The similarity ($f1$) and difference ($f2$) factors were calculated according to the following equations:

$$f1 = \frac{\left[\sum_{(t=1,\ldots,n)} |Rt - Tt|\right]}{\left[\sum_{(t=1,\ldots,n)} Rt\right]} \times 100;$$

$$f2 = 50 \times \log\left\{\left[1 + \sum_{(t=1,\ldots,n)} (Rt - Tt)^2\right]^{-0.5} \times 100\right\}$$

where Rt and Tt are the percent of drug dissolved at each time point t for the dissolution profile of the reference and tested starch matrices, respectively, n is the sampling number.

The similarity factor ($f2$) of 50–100 ensures sameness of two products and difference factor ($f1$) of 0–15 ensures minor difference between two products (Costa & Sousa Lobo, 2001). All statistical analyses were performed with a 95% confidence level.

In order to find correlations between the kinetic parameters (k) of theophylline release and surface properties of the matrices obtained, the Pearson correlation test was conducted using IBM SPSS Statistics v.22.

3. Results and discussion

3.1. In vitro release study of T_f from HHP-treated and STR starch matrices

The results obtained were presented as T_f release profiles from the HP-treated and STR matrices (Figs. 1 and 2). The results indicated the percentage (cumulative) of T_f dissolved into the medium in relation to drug dose *i.e.* 10 mg (T_{f10}) and 50 mg (T_{f50}) per 0.5 g of starch.

The HP-treated matrices of MS, SS and Hylon at T_{f10} demonstrated dynamic release of the drug in the first stage (30 min) of analysis (Fig. 1A). The MS and SS matrices dissolved 90% and 73% of T_f, respectively already within the initial 30 min of the study. The maximum quantity (Q_{max}) of released T_f reaching 100% was demonstrated for MS matrix in the 60 min of the study. Likewise, the Q_{max} of released drug from the SS matrix reached 100%, however it was determined in the 120 min of analysis. The Q_{max} value received for Hylon matrix was also found in the 120 min of the measurement but it amounted to 95%. The results indicated that 5% of T_f remained in the formulation of Hylon matrix, and were not released with prolonged time.

A moderate and sustained T_f release was observed in the case of HP-treated matrices of amylopectin starches (WMS and AS) at T_{f10} (Fig. 1A). In opposite to MS, SS and Hylon matrices, the matrix obtained from pressurized WMS and AS dissolved significantly lower amount of drug throughout the 240 min of dissolution study. The Q_{max} values (87% and 85%, $p > 0.05$) of dissolved T_f were determined for WMS and AS matrix, respectively, in the 240 min of measurement.

Significant differences in the amount of released T_f were found between HP-treated MS and SS matrices (70% and 56%, respectively, $p < 0.05$) at T_{f50} within the first 30 min of the study (Fig. 1B). Approximately 20% less of T_f was dissolved from the amylopectin starch matrices upon that time as compared to the drug amount obtained at lower concentration. The Q_{max} of T_f dissolved from MS and SS matrices exceeded the level of 80% ($p > 0.05$), and it was determined already in the 90 min of analysis. An increase in T_f concentration in Hylon matrix affected significantly drug release after 90 min of the study as compared to the amount obtained at T_{f10}. Considering the Q_{max} values obtained for MS, SS and Hylon matrices ($p > 0.05$),

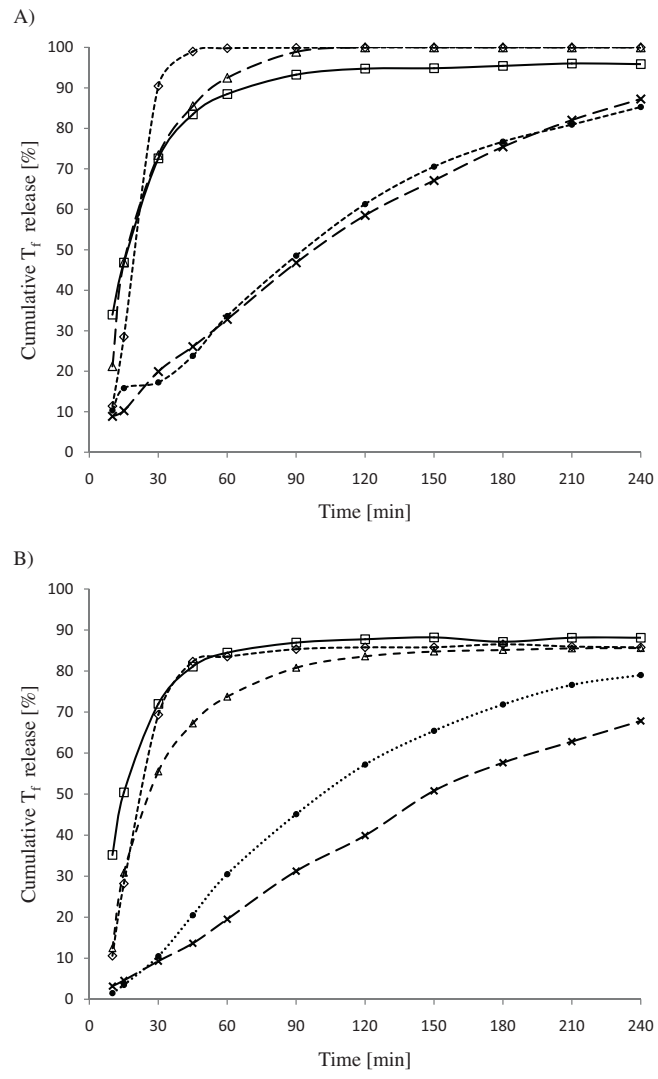

Fig. 1. Release profiles of theophylline at T_{f10} (A) and T_{f50} (B) from HP-treated starch matrices:
MS; Hylon; SS; WM; AS;

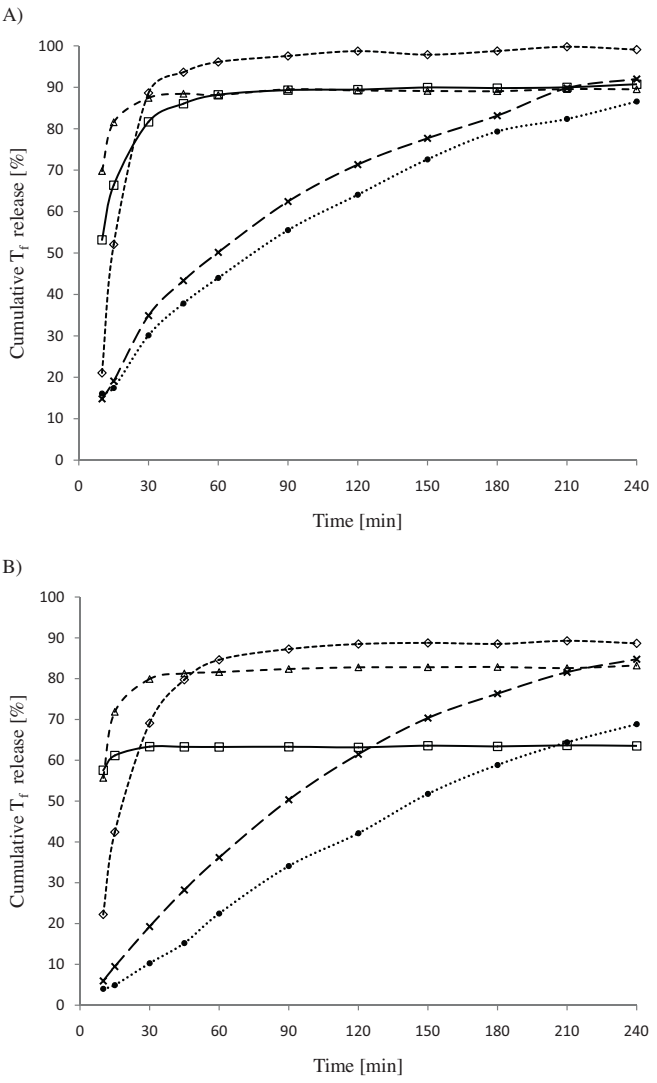

Fig. 2. Release profiles of theophylline at T_{f10} (A) and T_{f50} (B) from STR starch matrices:
MS; Hylon; SS; WM; AS;

it could be concluded that approximately 15% and 13% of T_f was not dissolved from these formulas during the remaining 150 min of analysis, respectively.

Irrespective of the applied T_f dose, the HP-treated WMS and AS matrices showed sustained drug release throughout the 240 min of analysis (Fig. 1A and B). An increase in T_f dose (T_{f50}) resulted in a significant decrease in drug release with emphasis on pressurized WMS matrix. While, 40% less T_f was dissolved from WMS matrix after the first 60 min of dissolution study, than approximately 20% less drug was released within the remaining 150 min of the study as compared to drug amount obtained at T_{f10}. On the contrary, the AS matrix released only by average 7% less of the drug during the remaining 180 min of analysis in relation to the amount obtained at lower T_f concentration. The Q_{max} values determined for WMS and AS matrices at the end of analysis reached 68% and 79%, respectively ($p < 0.05$).

Almost all the trends referred above have been met in the case of STR starch matrices at both T_f doses (T_{f10}, T_{f50}) (Fig. 2A and B). T_f release profiles of STR MS, SS and Hylon matrices presented a similar character as compared to the HP-treated matrices. Higher values of dissolved drug with emphasis on the first stage of the study were found for STR matrices, irrespective of T_f dose. It was also found that Q_{max} values reached by the STR matrices occurred at distinctly shorter time, however they were lower (with emphasis on SS and Hylon matrix) as compared to the Q_{max} values obtained for pressurized matrices. Of all the analyzed matrices, the STR Hylon matrix at T_{f50} manifested the weakest ability to release drug throughout the whole release study.

As in the case of HP-treated WMS and AS matrices, the STR matrices of amylopectin starches also formed a separate group of release profiles. The process applied (HP/STR) and the T_f dose in the formula differentiated considerably T_f dissolution ($p < 0.05$) between the WMS and AS matrices. Irrespective of drug dose, the STR matrix of WMS released significantly higher amount of drug than the HP-treated matrix. On the contrary, the STR matrix of AS released distinctly lower amount of drug than the pressurized matrix but this phenomenon was only found at higher T_f concentration. At higher T_f concentration less amount of drug was dissolved from both these STR matrices.

The formation of a satisfactory sustained-release matrix is strongly affected by the proportion and the structural characteristics of amylose and amylopectin. These two factors are crucial not only for matrix structure formation, but also for its viscoelastic properties, which among others, determine matrix diffusivity and drug release. Besides the branched structure, the much higher

Table 1
Fit factor values (*f*1, *f*2) obtained for the group of amylose starch matrices *vs* STR MS matrix.

Reference	Factor	HP MS	HP SS	HP Hylon	STR SS	STR Hylon
STR MS	T_{f10}					
	*f*1	5.57	4.18	7.80	15.73	12.87
	*f*2	54.59	62.18	54.86	36.35	44.19
	T_{f50}					
	*f*1	5.48	10.11	3.63	13.58	29.91
	*f*2	61.04	53.25	65.71	41.87	31.34

molecular weight of amylopectin than that of amylose was also important for the formation of a viscous and stable matrix (Onofre, Wang, & Mauromoustakos, 2009). Bearing in mind that Hylon starch below 140 °C formed unstable gel structure with poor viscoelastic properties (Vesterinen, Suortti, & Autio, 2001), we may speculate that the above mentioned phenomenon could be related to a fact that the STR Hylon matrix demonstrated rapid and uncontrolled T_f release.

The results obtained are consistent with literature data indicating that not only the composition and structure of starch matrix but also the T_f dose influenced the drug release (Szepes et al., 2008). The T_f concentration used in the aforementioned reference was slightly lower (40 mg/0.5 g starch dm) compared to the concentration applied in our experiment (50 mg/0.5 g starch dm). However, in opposite to our studies, Szepes and co-authors found that HP-treaded (700 MPa/5 min) matrices of potato and maize starch released distinctly lower amount of T_f. The maximum quantity of released T_f found by these authors for the HP-treated potato and maize matrices was approximately 45% and 15%, respectively. Even if matrix (formula) analyzed showing controlled release pattern, and the drug dissolution is distinctly inefficient, it should not be considered as a carrier for controlled drug delivery (Singh & Nath, 2013).

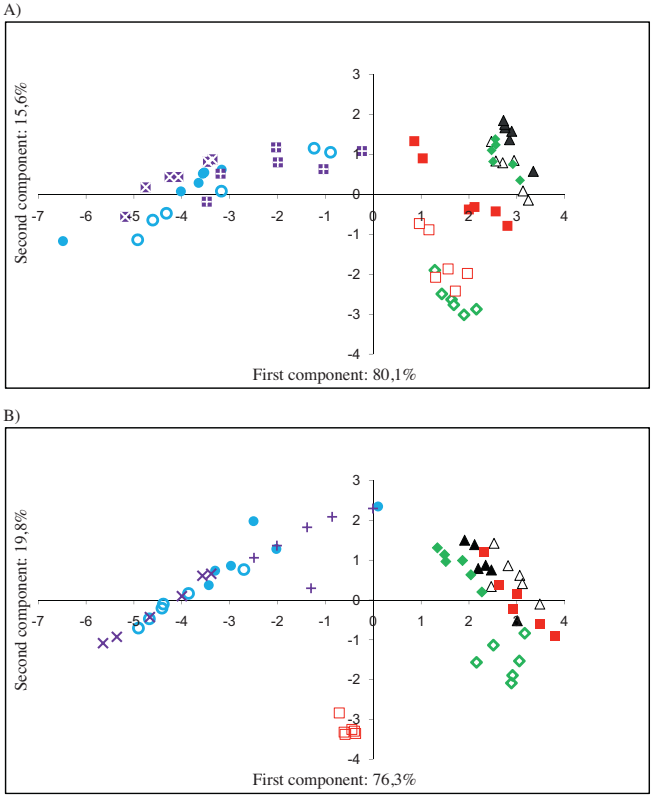

Fig. 3. Principal component analysis (PCA): score plot of HP and STR starch matrices at T_{f10} (A) and T_{f50} (B) ($n = 6$). ▲ MS-HP; △ MS-STR; ◆ SS-HP; ◇ SS-STR; ■ Hylon-HP; □ Hylon-STR; ● AS-HP; ○ AS-STR; ✕ WMS-HP; + WMS-STR. (For interpretation of the references to color in this figure legend, the reader is referred to the web version of this article.)

3.2. The principal component analysis (PCA) and release profile comparison

The principal component analysis (PCA) of T_f release profile from the starch matrices studied at given drug dose was presented in Fig. 3. The PCA carried out at T_{f10} (Fig. 3A) showed that the first two components can explain a total of 95.7% of variation in the data set (PC1—80.1%, PC2—15.6%). Whereas, at T_{f50}, the PC1 and PC2 explained 76.3% and 19.8% of the variance, respectively (Fig. 3B).

The score plots of the first two principal components showed separation of starch matrices into two groups in terms of amylose and amylopectin content (regardless of the treatment). The first group of amylose starch matrices was mainly in the positive sector, whereas the group of amylopectin matrices was in the negative sector of the diagrams presented (Fig. 3A and B). The second principal component (PC2) segregated starch matrices into two groups, as well. However, that phenomenon was observed only in the case of amylose starch matrices indicating the influence of treatment applied on drug dissolution with emphasis on the SS and Hylon matrix.

In view of the above, release profiles were compared in the group of amylose starch matrices. Since the MS is well characterized and used in the drug formulation (Adebayo, Brown-Myrie, & Itiola, 2008), the STR MS matrix was taken as a reference sample. The obtained values of *f*1 and *f*2 (Table 1) distinctly demonstrated that

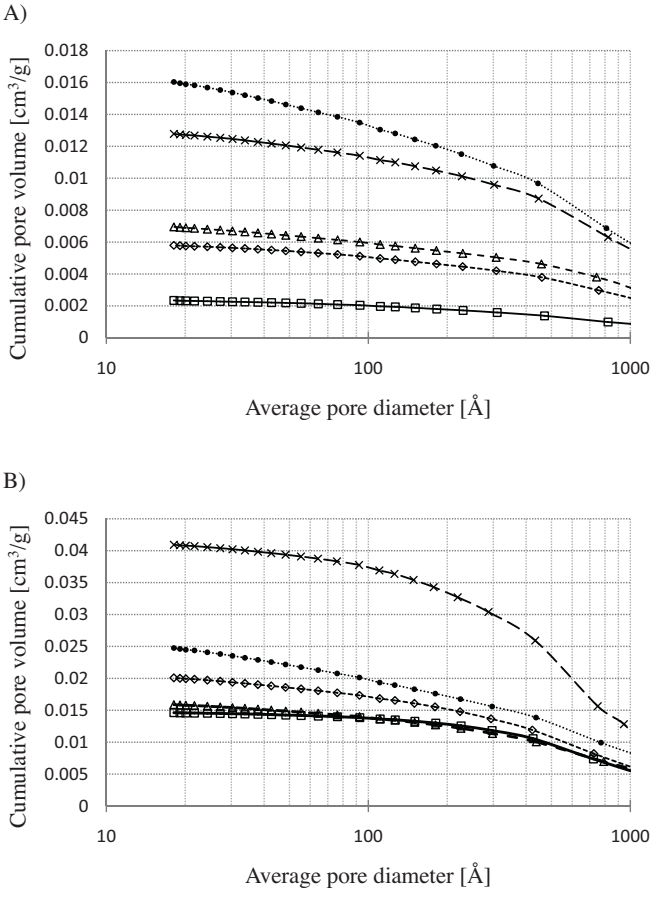

Fig. 4. Cumulative pore volume of HP (A) and STR (B) starch matrices using BJH desorption: MS; Hylon; SS; WM; AS;

Table 2
Comparative release kinetic parameters of HP-treated starch matrices.

Matrix	First order		Higuchi		Hixson–Crowell		Krosemeyer and Peppas	
	R	*k*	*R*	*k*	*R*	*k*	*R*	*n*
	T_{f10}							
MS	0.9248	4.23	0.5419	8.43	0.0000	0.60	0.7615	0.2646
SS	0.9882	3.99	0.5905	8.30	0.7744	0.56	0.8711	0.2586
Hylon	0.9862	4.06	0.2375	7.98	0.0000	0.38	0.8949	0.2244
WMS	0.9970	0.75	0.9699	5.28	0.9996	0.21	0.9975	0.7080
AS	0.9940	0.77	0.9690	5.33	0.9943	0.21	0.9912	0.6792
	T_{f50}							
MS	0.8977	2.82	0.6142	7.18	0.0000	0.29	0.8058	0.2748
SS	0.9248	2.06	0.7964	6.88	0.4228	0.27	0.8992	0.3150
Hylon	0.8497	3.92	0	7.46	0.0000	0.30	0.8672	0.1888
WMS	0.9935	0.45	0.9315	3.84	0.9976	0.13	0.9956	0.8886
AS	0.9906	0.66	0.9406	4.87	0.9919	0.18	0.9835	0.7811

Table 3
Comparative release kinetic parameters of STR starch matrices.

Matrix	First order		Higuchi		Hixson–Crowell		Krosemeyer and Peppas	
	R	*k*	*R*	*k*	*R*	*k*	*R*	*n*
	T_{f10}							
MS	0.9623	4.89	0.0000	8.38	0.0000	0.46	0.7969	0.2182
SS	0.0000	10.88	0.0000	7.90	0.0000	0.32	0.7912	0.0509
Hylon	0.6593	6.47	0.0000	7.81	0.0000	0.32	0.8614	0.1177
WMS	0.9919	0.75	0.9934	6.22	0.9742	0.26	0.9934	0.4980
AS	0.9879	0.92	0.9963	5.73	0.9719	0.22	0.9968	0.5213
	T_{f50}							
MS	0.9264	3.28	0.4366	7.43	0.0000	0.31	0.8556	0.2389
SS	0.0000	6.74	0.0000	7.28	0.0000	0.27	0.7915	0.0774
Hylon	0.0000	1.34	0.0000	5.66	0.0000	0.18	0.7720	0.0209
WMS	0.9991	0.78	0.9315	3.84	0.9944	0.21	0.9915	0.6745
AS	0.9965	0.74	0.9406	4.87	0.9985	0.14	0.9957	0.8378

the dissolution profiles of STR SS and STR Hylon (at both T_f doses) can be considered different compared to the reference matrix and to the other matrices analyzed.

Considering data obtained, it may be concluded that: (i) the botanical origin of starch (amylose/amylopectin content) affects drug dissolution from the starch matrices studied; (ii) irrespective of treatment, the amylopectin starch matrices showed homogeneity in T_f dissolution; and (iii) drug dissolution from SS and Hylon matrices was affected to a greater extent by processing applied than by amylose content.

3.3. Kinetics and mechanism of T_f release

The kinetic parameters describing the mechanism of T_f release from the starch matrices studied were presented in Tables 2 and 3. The release rate constant (K) was calculated from the slope of the appropriate equations and the correlation coefficient (R) was determined for all the matrices containing T_f.

Of all the analyzed matrices, only the amylopectin starches (HP and STR) at both drug doses showed the highest R value and acceptable K value (low). According to Singh and Nath (2013), the kinetic parameters obtained indicated a controlled release mechanism of T_f from the amylopectin starch matrices.

In details, the *in vitro* drug release from the HP-treated amylopectin starch matrices at both drug doses (T_{f10} and T_{f50}), was best fitted and explained by the Hixson–Crowell model with the highest linearity (R = 0.994–0.999), first order kinetics (R = 0.994–0.997), Korsmeyer–Pepas model (R = 0.991–0.998), and finally Higuchi model (R = 0.969–0.970) (Table 2). The release mechanism of T_f characterized by the Hixson–Crowell model indicated that the dissolution occurred only in vertical direction relative to the matrix surface (Szepes et al., 2008). Moreover, matrix shape was not triggered by the T_f release process.

The results of the fitting of release profiles of STR matrices were summarized in Table 3. Also in that case, the highest correlation values were obtained for WMS and AS matrices. However, the kinetics of T_{f10} release from these matrices were as follows: Higuchi = Korsmeyer–Pepas < first order kinetics < Hixson–Crowell. On the contrary, the lowest R values were found for the Higuchi model when fitting the dissolution profiles at higher T_f dose (T_{f50}). The best fit was obtained for the first order kinetics, Hixson–Crowell model and finally for the Korsmeyer–Pepas model.

Bearing in mind that the drug release kinetics might be also diffusion/erosion controlled (Lao, Peppas, Boey, & Venkatraman, 2011), and/or swelling (Lopez-Cordoba et al., 2014), the Korsmeyer–Pepas model is useful to evaluate the mechanism

Table 4
BET surface area, average pore size of HP-treated and STR starch matrices.

Starch	Surface area (m^2/g)		Pore diameter by BJH (Å)		Pore diameter by SEM (μm)	
	HP	STR	HP	STR	HP	STR
MS	1.6303	5.8638	179	157	3.1 ± 1.9	1.9 ± 1.0
SS	1.9622	4.3017	164	177	1.6 ± 1.3	2.0 ± 1.0
Hylon	0.6314	2.7328	162	198	–	–
WMS	3.2956	8.6178	192	229	4.9 ± 1.7	1.0 ± 0.5
AS	5.1023	8.5255	147	133	1.4 ± 0.6	1.1 ± 0.5

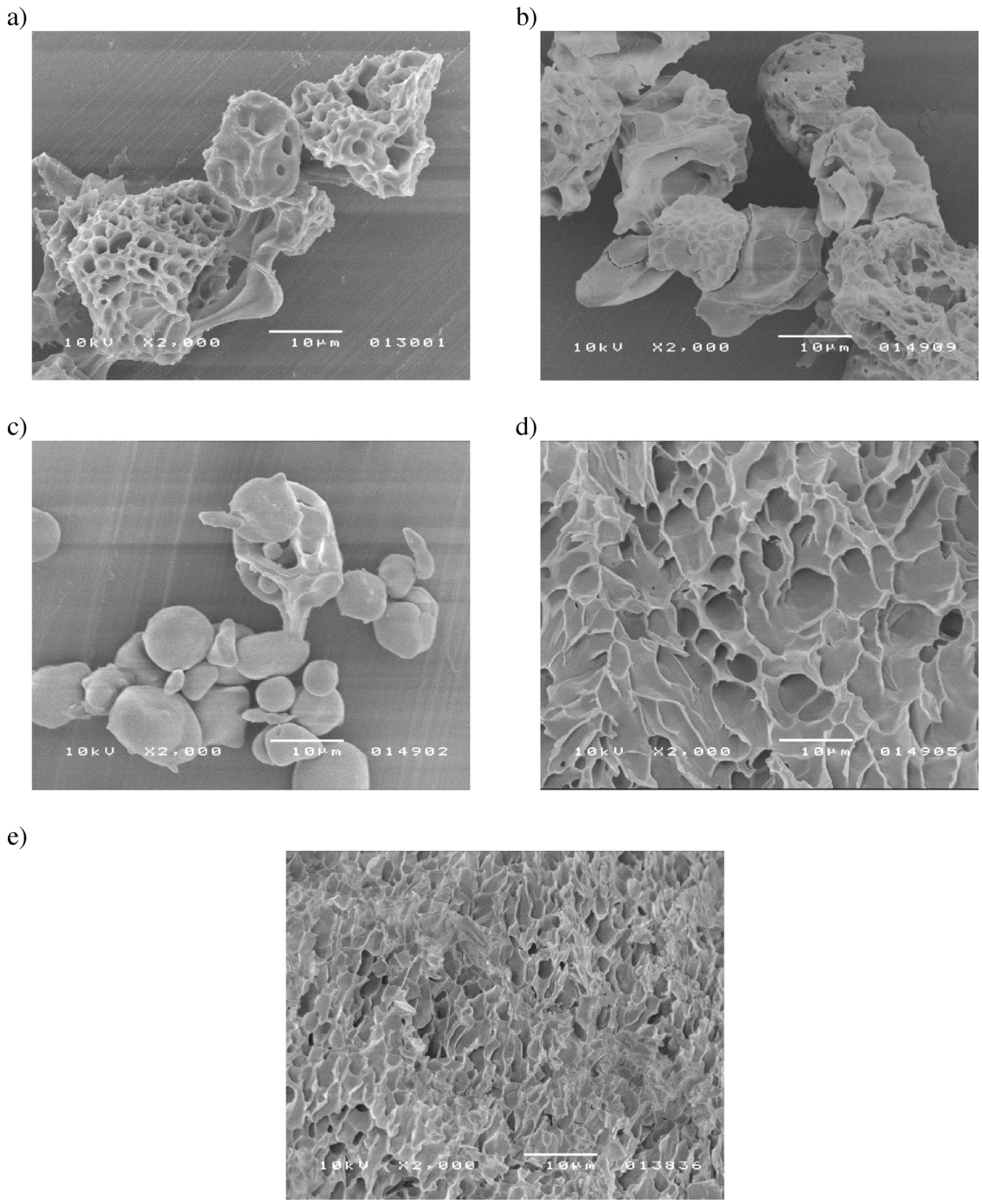

Fig. 5. SEM micrographs of HP-treated starch matrices: (a) MS; (b) SS; (c) Hylon; (d) WMS; (e) AS.

of drug dissolution. The Korsmeyer–Pepas kinetic parameters as k and n are related to the release rate constant, and to the mechanism of drug release, respectively (Tables 2 and 3). Only in the case of STR WMS and AS matrices with lower T_f dose, the n parameter determined was 0.5, which indicated that drug release from the matrix occurred *via* the Fickian diffusion (Singh & Nath, 2013). Moreover, the Korsmeyer–Pepas equation (for $n = 0.5$) was equal to the square root model described by Higuchi. A higher n value than 0.5, found for HP-treated (T_{f10}, T_{f50}) and STR matrices (T_{f50}), signified non-Fickian and/or anomalous drug transport (Szepes et al., 2008). The anomalous transport consisted of both phenomena: drug diffusion in the hydrated matrix, and polymer relaxation (Nair & Jyothi, 2013). Considering these facts, it could be stated that the T_f release from the aforementioned matrices was an anomalous transport with non-Fickian kinetics coupling the diffusion process, matrix swelling and relaxation (Singh & Nath, 2013; Nair & Jyothi, 2013).

3.4. Surface properties and morphology (SEM) of starch matrices

In order to characterize the surface properties of starch matrices, the specific surface area and average pores diameter were estimated using low-temperature nitrogen adsorption (Table 4). Irrespectively of the processing applied, the values of surface area

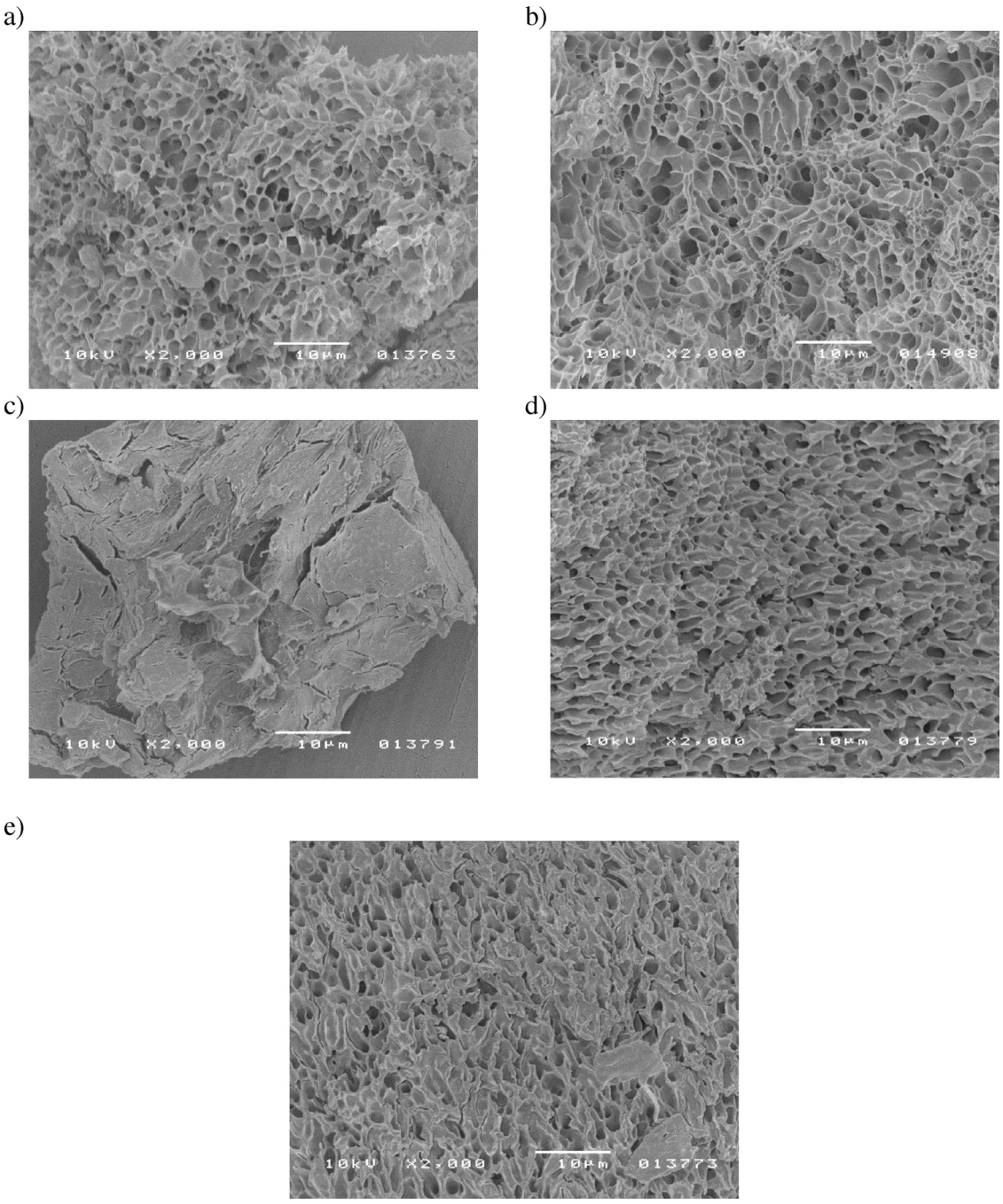

Fig. 6. SEM micrographs of STR starch matrices: (a) MS; (b) SS; (c) Hylon; (d) WMS; (e) AS.

determined for WMS and AS matrices were the highest, and for Hylon matrix—the lowest as compared to MS and SS matrices. The starch matrices showed explicit differences regarding the pore size, as well. Unquestionably, all the analyzed starch matrices revealed pores in the meso-to-macro scale. The processed AS matrix exhibited the smallest pores, whereas HP-treated WMS and STR Hylon matrices were characterized by the highest mesopores size compared to the others matrices. It is assumed that the internal surface area of polysaccharide hydrogels is formed by the nanopores or even smaller structures (Lynam et al., 2014).

In order to characterize the internal structure of starch matrices the BJH desorption model was used to define the total mesopores volume and to provide information on the pore size distribution (Fig. 4). The higher cumulative pore volume and higher concentration of smaller pores (*i.e.* 25–50 Å) were found for the starch matrices analyzed with emphasis on WMS and AS. The matrices produced *via* HP treatment exhibited significantly lower cumulative pore values (Fig. 4A) than the STR matrices (Fig. 4B).

As evidenced by SEM, the microstructure of starch matrices obtained *via* HP and STR distinctly varied (Figs. 5 and 6). The HP treatment of MS resulted in an advanced gelatinization of granules, which in turn affected their disruption and formation of the gel particles with porous surface (Fig. 5a). The majority of SS granules appeared distinctly affected by pressurization and demonstrated advanced swelling and surface erosion (Fig. 5b), whereas the Hylon starch retained granular shape after the treatment (Fig. 5c). The

microphotographs of WMS and AS matrices (Fig. 5d and e) can be considered distinctly different from one another, and compared to the aforementioned amylose starch matrices. Both the amylopectin matrices formed homogenous and continuous gel network. However, the gel network of AS matrix exhibited smaller and more uniform micropore sizes than the gel of WMS matrix (Table 4).

The STR process evoked changed in the matrix morphology (Fig. 6), which in turn resulted in a significant increase in the surface area (Table 4) or pore volume (Fig. 4). The SEM observations are in high accordance to the phenomenon of starch gelatinization under autoclaving condition showing that at the applied temperature (120 °C) there is indeed an end of this process. The autoclaving (STR) of MS, SS and Hylon led to formation of bicontinuous network consisting of highly solubilized amylose and amylopectin (Fig. 6a–c), whereas amylopectin of WMS and AS was, as in the case of HP, in a continuous form (Fig. 6d and e).

In order to find correlations between the kinetic parameters of theophylline release and surface properties of starch matrices, the Pearson correlation test was conducted. Since, the amylopectin starch matrices (HHP-treated and STR) effectively processed with selected mathematical models, the correlation was tested only for these matrices. The best fitted models were chosen *i.e.* the Hixson–Crowell model for HP-treated matrices, and the Higuchi model for STR matrices.

The Pearson test revealed moderate correlation ($r = 0.598$ and $p < 0.05$) between parameter k (Higuchi release rate constant) and the surface area only in case of STR matrices (Tables not shown). Moreover, these matrices also showed stronger correlation between surface area and pore diameter (BJH) ($r = 0.744$, $p < 0.01$). In case of matrices obtained *via* HP treatment, negative and high correlation was found between surface area – pore diameter (BJH) ($r = -1$) as well as surface area – pore diameter (SEM) ($r = -0.846$, $p < 0.01$).

These data confirmed that both processes used *i.e.* HP and STR significantly affected the surface properties and morphology of the matrices however to a different extent (Table 4, Figs. 5 and 6). It was also indicated that the starch matrix structure and its composition were key factors influencing matrix properties, and finally T_f diffusion process.

4. Conclusion

The proper selection of starch source and applicability of physical treatment give rise to obtain a starch-based matrix with the ability to provide controlled release of theophylline. In this study we correlated the effect of starch granule composition, HP-treatment and STR with the T_f release (dynamics/kinetics). Specifically, it was found that the botanical origin of starch (amylose/amylopectin content) determined the matrix structure, internal surface area and porosity, and therefore can be considered as a key factor affecting the T_f release. Irrespective of treatment, only the amylopectin starch matrices exhibited a controlled drug release. However, the mechanism of T_f release was strictly related to the processing applied and drug concentration. At lower T_f dose, drug release from the STR WMA and AS matrix occurred *via* the Fickian diffusion. The lower surface area and pore volume found for HP-treated amylopectin could be responsible for the phenomenon of non-Fickian and/or anomalous drug transport in these matrices.

Acknowledgement

The study was financed by a grant of the Polish Ministry of Science and Higher Education (Grant no. N N312 101938).

References

Adebayo, S. A., Brown-Myrie, E., & Itiola, O. A. (2008). Comparative disintegrant activities of breadfruit starch and official corn starch. *Powder Technology*, *181*, 98–103.

Barrett, E. P., Joyner, L. G., & Hallenda, P. H. (1951). The determination of pore volume and area distributions in porous substances. I. Computations from nitrogen isotherms. *Journal of the American Chemical Society*, *73*, 373–381.

Bialleck, S., & Rein, H. (2011). Preparation of starch-based pellets by hot-melt extrusion. *European Journal of Pharmaceutics and Biopharmaceutics*, *79*, 440–448.

Błaszczak, W., Wasserman, L. A., Fornal, J., & Yuryev, V. P. (2007). Effect of high hydrostatic pressure on the structure and gelling properties of amylopectin maize, wheat and potato starches. *Polish Journal of Food and Nutrition Sciences*, *57*, 475–480.

Błaszczak, W., Misharina, T. A., Fessas, D., Signorelli, M., & Górecki, A. R. (2013). Retention of aroma compounds by corn, sorghum and amaranth starches. *Food Research International*, *54*, 338–344.

Brunauer, S., Emmett, P. H., & Teller, E. (1938). Adsorption of gases in multimolecular layers. *Journal of American Chemical Society*, *60*, 309–319.

Costa, P., & Sousa Lobo, J. M. (2001). Modeling and comparison of dissolution profiles. *European Journal of Pharmaceutical Sciences*, *13*, 123–133.

Ismail, H., Irani, M., & Ahmad, Z. (2013). Starch-based hydrogels: Present status and applications. *International Journal of Polymeric Materials and Polymeric Biomaterials*, *62*, 411–420.

Lao, L. L., Peppas, N. A., Boey, F. Y. C., & Venkatraman, S. S. (2011). Modeling of drug release from bulk-degrading polymers. *International Journal of Pharmaceutics*, *418*, 28–41.

Lopez-Cordoba, A., Deladino, L., & Martino, M. (2014). Release of yerba mate antioxidants from caorn starch-alginate capsules as affected by structure. *Carbohydrate Polymers*, *99*, 150–157.

Lynam, D., Peterson, C., Maloney, R., Shahriari, D., Garrison, A., Saleh, S., et al. (2014). Augmenting protein release from layer-by-layer functionalized agarose hydrogels. *Carbohydrate Polymers*, *103*, 377–384.

Nair, S. B., & Jyothi, A. (2013). Cassava starch-konjac glucomannan biodegradable blend films: In vitro study as a matrix for controlled drug delivery. *Starch*, *65*, 273–284.

Olayinka, O. O., Adebowale, K. O., & Olu-Owolabi, B. I. (2008). Effect of heat–moisture treatment on physicochemical properties of white sorghum starch. *Food Hydrocolloids*, *22*, 225–230.

Onofre, F., Wang, Y-J., & Mauromoustakos, A. (2009). Effect of structure and modification on sustained release properties of starches. *Carbohydrate Polymers*, *76*, 541–547.

Pei-Ling, L., Qing, Z., Qun, S., Xiao-Song, H., & Ji-Hong, W. (2012). Effect of high hydrostatic pressure on modified noncrystalline granular starch of starches with different granular type and amylose content. *LWT—Food Sciences and Technology*, *47*, 450–458.

Singh, A. V., & Nath, L. K. (2013). Evaluation of chemically modified hydrophobic sago starch as a carrier for controlled drug delivery. *Saudi Pharmaceutical Journal*, *21*, 193–200.

Szepes, A., Makai, Z., Blumer, C., Mader, K., Kasa, P., Jr., & Szabo-Revesz, P. (2008). Characterization and drug delivery behavior of starch-based hydrogels prepared via isostatic ultrahigh pressure. *Carbohydrate Polymers*, *72*, 571–578.

Vallons, K. J. R., & Arendt, E. K. (2009). Effects of high pressure and temperature on buckwheat starch characteristics. *European Food Research and Technology*, *230*, 343–351.

Vesterinen, E., Suortti, T., & Autio, K. (2001). Effects of preparation temperature on gelation properties and molecular structure of high-amylose maize starch. *Cereal Chemistry*, *78*, 442–446.

Walkowski, A., Fornal, J., Lewandowicz, G., & Sadowska, J. (1997). Structure, physicochemical properties and potential uses of amaranth starch. *Polish Journal of Food and Nutrition Sciences*, *6*, 11–22.

Wolny, D., Gruchlik, A., Chodurek, E., Szara, M., & Dzierżewicz, Z. (2012). Comparison of dissolution profiles of theophylline extended-release dosage forms. *Acta Poloniale Pharmaceutica—Drug Research*, *69*, 1384–1386.

Xiao, C. (2013). Current advances of chemical and physical starch-based hydrogels. *Starch*, *65*, 82–88.

Yoon, H. S., Lee, J. H., & Lim, S. T. (2009). Utilization of retrograded waxy maize starch gels as tablet matrix for controlled release of theophylline. *Carbohydrate Polymers*, *76*, 449–453.